数理解析研究所講究録
914巻 1995年 48-68

Flow induced around a sphere with a nonuniform surface temperature in a rarefied gas, with application to the drag and thermal force problems of a spherical particle with an arbitrary thermal conductivity

S. TAKATA and Y. SONE

京大・工・航空宇宙　　高田 滋,　曾根 良夫

Division of Aeronautics and Astronautics, Graduate School of Engineering, Kyoto University, Kyoto 606-01, Japan.

Abstract

A flow induced around a sphere with a nonuniform surface temperature in a rarefied gas is investigated on the basis of the linearized Boltzmann equation for hard-sphere molecules and diffuse reflection condition. With the aid of the accurate and efficient numerical method developed by the authors with Aoki [S. Takata, Y. Sone, and K. Aoki, *Phys. Fluids A*, **5**, 716 (1993)], the behavior of the gas, the velocity distribution function as well as macroscopic variables and force on the sphere, is clarified for the whole range of the Knudsen number. In addition, the solutions of the drag and thermal force (thermophoresis) problems of a spherical particle with an arbitrary thermal conductivity are obtained by appropriate superpositions of the present solution and those of a sphere with infinite thermal conductivity, obtained by the authors with Aoki. The result of the thermal force is compared with various experimental data.

I. Introduction

Gas dynamics problems in a small system, as well as those of a rarefied gas, which are important in aerosol science and micromachine engineering, require kinetic theory analysis, since the mean free path is comparable to the small characteristic length of the system. When the kinetic effect or the effect of rarefaction of a gas is important, the temperature field and solid walls, though at rest, have important effects on gas motion. For small Knudsen numbers, according to the asymptotic theory[1–5], developed by a systematic analysis of the Boltzmann equation, the temperature and wall effects on gas motion, such as thermal creep flow[6–8], thermal stress slip flow[9,10], and nonlinear thermal stress flow[11], are characterized by the local behavior of the system. For intermediate and large Knudsen numbers, these effects are not characterized only by the local behavior, such as the temperature gradient of the wall in the thermal creep flow, and global geometry of the system is also important. Thus, analyses of various typical systems are useful for general understanding. In the present paper we take the system where a sphere with a nonuniform surface temperature is placed in a uniform gas at rest, and investigate the behavior of the gas, especially the flow induced around the sphere and the force on the sphere, for the whole range of the Knudsen number on the basis of the standard Boltzmann equation for hard-sphere molecules. The numerical method adopted in the analysis is a combination of the hybrid-finite-difference method, capable of describing the discontinuity of the velocity distribution function in the gas, and the numerical kernel method, an efficient method of computation of the collision integral, in Ref. 12.

The problem has important applications to analyses of the drag and thermal force problems of a spherical particle with an arbitrary thermal conductivity. The drag problem (Problem D, for short) is concerned with a particle in a uniform flow of a gas, and the thermal force (thermophoresis) problem (Problem T, for short) is concerned with a particle in a gas at rest with a uniform temperature gradient. These problems, important in aerosol science, have been studied by various authors (e.g., Refs. 13–27, 12 for problem D; Refs. 28–35, 9, 36–44, 10, 45–47 for problem T; and Refs. 48–53 for both problems). It is, however, recent that the problems are analyzed accurately for the whole range of the Knudsen number on the basis of the standard Boltzmann equation. That is, in Refs. 12 and 47, the problems D and T for a sphere with a uniform surface temperature

are analyzed numerically on the basis of the Boltzmann equation for hard-sphere molecules. The results apply only to the drag and thermal force problems for a spherical particle with infinite thermal conductivity. The drag or thermal force problem for a spherical particle with an arbitrary thermal conductivity, as will be shown in Sec. VI, can be decomposed into two problems: problem D or T for a sphere with a uniform surface temperature and the problem of a sphere with a nonuniform temperature, and the solution is obtained as an appropriate superposition of the two problems. This is another reason that we consider the problem of a sphere with a nonuniform surface temperature in this paper.

II. Problem and notations

In Secs. III–V, we consider a spherical body with a nonuniform surface temperature [radius L and surface temperature $T_w = T_0(1 + \alpha X_1/L)$, where X_i is a Cartesian coordinate system with its origin at the center of the sphere and α is a constant] in a rarefied gas at rest (pressure p_0 and temperature T_0), and investigate the steady flow induced around the sphere and the force on the sphere under the following assumptions:
(i) The gas molecules are hard spheres of a uniform size and undergo complete elastic collisions between themselves.
(ii) The gas molecules are reflected diffusely on the sphere.
(iii) The magnitude of the temperature variation α is so small that the equation and the boundary condition can be linearized around the uniform equilibrium state at rest with pressure p_0 and temperature T_0.
Then, in Sec. VI we consider the drag and thermal force problems for a spherical particle with an arbitrary thermal conductivity.

We summarize other main notations used in this paper: $\rho_0 = p_0/RT_0$; R (the specific gas constant) is defined by the Boltzmann constant divided by the mass of the molecule; ℓ_0 is the mean free path of the gas molecules at the equilibrium state at rest with pressure p_0 and temperature T_0 [for a hard-sphere molecular gas, $\ell_0 = (\sqrt{2}\pi\sigma^2\rho_0/m)^{-1}$, where σ and m are, respectively, the diameter and mass of the molecule]; $Kn = \ell_0/L$ (Knudsen number); $k = (\sqrt{\pi}/2)Kn$; $x_i = X_i/L$; (r, θ, φ) is the polar coordinate system in the x_i space with $r = 0$ at $x_i = 0$ and with $\theta = 0$ (the polar direction) in the x_1 direction; $(2RT_0)^{1/2}\zeta_i$ is the molecular velocity; $\zeta = |\zeta_i| = (\zeta_i^2)^{1/2}$; ζ_r and ζ_θ are, respectively, the r and θ components of ζ_i; $E(\zeta) = \pi^{-3/2}\exp(-\zeta^2)$; $\rho_0(2RT_0)^{-3/2}E(\zeta)(1+\phi)$ is the velocity distribution function of the gas molecules; $\rho_0(1+\omega)$ is the density of the gas; $T_0(1+\tau)$ is the temperature; $p_0(1 + P)$ is the pressure; $(2RT_0)^{1/2}u_i$ is the flow velocity; $p_0(\delta_{ij} + P_{ij})$ is the stress tensor, where δ_{ij} is the Kronecker delta; and $p_0(2RT_0)^{1/2}Q_i$ is the heat flow vector. The components of u_i, P_{ij}, and Q_i in the (r, θ, φ) system are expressed by the subscripts r, θ, and φ (e.g., u_r, u_θ). $T_w[= T_0(1 + \tau_w)$, $\tau_w = \alpha\cos\theta]$ is the surface temperature of the sphere. (Fig. 1)

III. Basic equation and boundary condition

The linearized Boltzmann equation for a steady state is written as

$$\zeta_i\frac{\partial\phi}{\partial x_i} = \frac{1}{k}\mathcal{L}(\phi). \tag{1}$$

The linearized collision integral $\mathcal{L}(\phi)$ is expressed in the following form for hard-sphere molecules[54,55]:

$$\mathcal{L}(\phi) = \mathcal{L}_1(\phi) - \mathcal{L}_2(\phi) - \nu(\zeta)\phi, \tag{2}$$

$$\mathcal{L}_1(\phi) = \frac{1}{\sqrt{2}\pi}\int\frac{1}{|\zeta_i - \xi_i|}\exp\left(-\xi_j^2 + \frac{|\zeta_i \wedge \xi_i|^2}{|\zeta_i - \xi_i|^2}\right)\phi(x_i, \xi_i)d\xi_1 d\xi_2 d\xi_3, \tag{3a}$$

$$\mathcal{L}_2(\phi) = \frac{1}{2\sqrt{2}\pi} \int |\zeta_i - \xi_i| \exp(-\xi_j^2) \phi(x_i, \xi_i) d\xi_1 d\xi_2 d\xi_3, \tag{3b}$$

$$\nu(\zeta) = \frac{1}{2\sqrt{2}} \left[\exp(-\zeta^2) + (2\zeta + \frac{1}{\zeta}) \int_0^\zeta \exp(-\xi^2) d\xi \right], \tag{3c}$$

where $\zeta_i \wedge \xi_i$ is the vector product of ζ_i and ξ_i.

The linearized form of the diffuse reflection condition on the sphere ($x_i^2 = 1$) is given by

$$\phi(x_i, \zeta_i) = (\zeta^2 - 2)\alpha x_1 - 2\pi^{1/2} \int_{\zeta_i n_i < 0} \zeta_j n_j \phi \mathrm{E}\, d\zeta_1\, d\zeta_2\, d\zeta_3, \quad (\zeta_i n_i > 0), \tag{4}$$

where n_i is the unit normal vector to the boundary, pointed to the gas. The condition at infinity is

$$\phi \to 0. \tag{5}$$

The (nondimensional) macroscopic variables ω, τ, u_i, etc. are given as the moments of ϕ:

$$\omega = \int \phi \mathrm{E}\, d\zeta_1\, d\zeta_2\, d\zeta_3, \tag{6a}$$

$$u_i = \int \zeta_i \phi \mathrm{E}\, d\zeta_1\, d\zeta_2\, d\zeta_3, \tag{6b}$$

$$\tau = \frac{2}{3} \int (\zeta_j^2 - \frac{3}{2}) \phi \mathrm{E}\, d\zeta_1\, d\zeta_2\, d\zeta_3, \tag{6c}$$

$$\mathrm{P} = \omega + \tau, \tag{6d}$$

$$\mathrm{P}_{ij} = 2 \int \zeta_i \zeta_j \phi \mathrm{E}\, d\zeta_1\, d\zeta_2\, d\zeta_3, \tag{6e}$$

$$\mathrm{Q}_i = \int \zeta_i (\zeta_j^2 - \frac{5}{2}) \phi \mathrm{E}\, d\zeta_1\, d\zeta_2\, d\zeta_3. \tag{6f}$$

The boundary-value problem (1), (4), and (5) with six independent variables x_i and ζ_i can be reduced to a problem of a simultaneous integrodifferential system with three independent variables. That is, the solution of Eqs. (1), (4), and (5) is expressed by the following similarity solution[41]:

$$\phi = \Phi_c(r, \zeta, \theta_\zeta) \cos\theta + \zeta_\theta \Phi_s(r, \zeta, \theta_\zeta) \sin\theta, \tag{7}$$

$$\theta_\zeta = \pi - \mathrm{Arccos}\,(\zeta_r/\zeta), \qquad (0 \le \theta_\zeta \le \pi), \tag{8}$$

where $\pi - \theta_\zeta$ is the angle between the molecular velocity ζ_i and the radial direction. The Φ_c and Φ_s are determined by the boundary-value problem:

$$\mathcal{D}\Phi_c + \frac{(\zeta \sin\theta_\zeta)^2}{r} \Phi_s = \frac{1}{k} \left[\mathcal{L}_1^c(\Phi_c) - \mathcal{L}_2^c(\Phi_c) - \nu(\zeta)\Phi_c \right], \tag{9}$$

$$\mathcal{D}(\Phi_s \zeta \sin\theta_\zeta) - \frac{\zeta \sin\theta_\zeta}{r} \Phi_c = \frac{1}{k} \left[\mathcal{L}_1^s(\Phi_s \xi \sin\theta_\xi) - \mathcal{L}_2^s(\Phi_s \xi \sin\theta_\xi) - \nu(\zeta)\Phi_s \zeta \sin\theta_\zeta \right], \tag{10}$$

and at $r = 1$

$$\begin{cases} \Phi_c = (\zeta^2 - 2)\alpha + 2\pi^{3/2} \displaystyle\int_0^\infty \int_0^{\pi/2} \zeta^3 \sin 2\theta_\zeta \Phi_c \mathrm{E}\, d\theta_\zeta\, d\zeta, & (\pi/2 \le \theta_\zeta \le \pi), \\ \Phi_s = 0, \end{cases} \tag{11}$$

and as $r \to \infty$,

$$\Phi_c \to 0, \qquad \Phi_s \to 0. \tag{12}$$

The operators $\mathcal{D}$, $\mathcal{L}_1^c$, etc. in Eqs. (9) and (10) are defined as follows:

$$\mathcal{D}\Phi = -\zeta\cos\theta_\zeta\frac{\partial\Phi}{\partial r} + \frac{\zeta\sin\theta_\zeta}{r}\frac{\partial\Phi}{\partial\theta_\zeta}, \tag{13}$$

$$\mathcal{L}_1^c(\Phi) = \frac{1}{\sqrt{2}\pi}\int_0^\infty\int_0^\pi\int_0^{2\pi}\frac{\xi^2\sin\theta_\xi}{\mathcal{F}_1}\exp\left(-\xi^2+\frac{\mathcal{F}_2}{\mathcal{F}_1^2}\right)\Phi(r,\xi,\theta_\xi)\,d\bar{\psi}\,d\theta_\xi\,d\xi, \tag{14a}$$

$$\mathcal{L}_2^c(\Phi) = \frac{1}{2\sqrt{2}\pi}\int_0^\infty\int_0^\pi\int_0^{2\pi}\mathcal{F}_1\xi^2\sin\theta_\xi\exp(-\xi^2)\Phi(r,\xi,\theta_\xi)\,d\bar{\psi}\,d\theta_\xi\,d\xi, \tag{14b}$$

$$\mathcal{L}_1^s(\Phi) = \frac{1}{\sqrt{2}\pi}\int_0^\infty\int_0^\pi\int_0^{2\pi}\frac{\xi^2\sin\theta_\xi\cos\bar{\psi}}{\mathcal{F}_1}\exp\left(-\xi^2+\frac{\mathcal{F}_2}{\mathcal{F}_1^2}\right)\Phi(r,\xi,\theta_\xi)\,d\bar{\psi}\,d\theta_\xi\,d\xi, \tag{15a}$$

$$\mathcal{L}_2^s(\Phi) = \frac{1}{2\sqrt{2}\pi}\int_0^\infty\int_0^\pi\int_0^{2\pi}\mathcal{F}_1\xi^2\sin\theta_\xi\cos\bar{\psi}\exp(-\xi^2)\Phi(r,\xi,\theta_\xi)\,d\bar{\psi}\,d\theta_\xi\,d\xi, \tag{15b}$$

$$\mathcal{F}_1 = \left[\zeta^2+\xi^2-2\zeta\xi(\cos\theta_\zeta\cos\theta_\xi+\sin\theta_\zeta\sin\theta_\xi\cos\bar{\psi})\right]^{1/2}, \tag{16a}$$

$$\mathcal{F}_2 = \zeta^2\xi^2\left[\cos^2\theta_\zeta\sin^2\theta_\xi+\sin^2\theta_\zeta\cos^2\theta_\xi+\sin^2\theta_\zeta\sin^2\theta_\xi\sin^2\bar{\psi}\right. \tag{16b}$$
$$\left.-2\cos\theta_\zeta\sin\theta_\zeta\cos\theta_\xi\sin\theta_\xi\cos\bar{\psi}\right].$$

The set $(\xi,\ \pi-\theta_\xi,\ \bar{\psi})$ corresponds to the polar coordinate expression of ξ_i in Eqs. (3a) and (3b), with the polar direction in the radial direction.

The macroscopic variables ω, u_r, u_θ, etc. are expressed by Φ_c and Φ_s as follows:

$$\omega = 2\pi\left(\int_0^\infty\int_0^\pi\zeta^2\sin\theta_\zeta\Phi_c\mathrm{E}d\theta_\zeta d\zeta\right)\cos\theta, \tag{17a}$$

$$u_r = -\pi\left(\int_0^\infty\int_0^\pi\zeta^3\sin 2\theta_\zeta\Phi_c\mathrm{E}d\theta_\zeta d\zeta\right)\cos\theta, \tag{17b}$$

$$u_\theta = \pi\left(\int_0^\infty\int_0^\pi\zeta^4\sin^3\theta_\zeta\Phi_s\mathrm{E}d\theta_\zeta d\zeta\right)\sin\theta, \tag{17c}$$

$$u_\varphi = 0, \tag{17d}$$

$$\tau = \frac{4}{3}\pi\left[\int_0^\infty\int_0^\pi\zeta^2(\zeta^2-\frac{3}{2})\sin\theta_\zeta\Phi_c\mathrm{E}d\theta_\zeta d\zeta\right]\cos\theta, \tag{17e}$$

$$\mathrm{P}_{rr} = 4\pi\left(\int_0^\infty\int_0^\pi\zeta^4\cos^2\theta_\zeta\sin\theta_\zeta\Phi_c\mathrm{E}\,d\theta_\zeta\,d\zeta\right)\cos\theta, \tag{17f}$$

$$\mathrm{P}_{\theta\theta} = 2\pi\left(\int_0^\infty\int_0^\pi\zeta^4\sin^3\theta_\zeta\Phi_c\mathrm{E}\,d\theta_\zeta\,d\zeta\right)\cos\theta, \tag{17g}$$

$$\mathrm{P}_{r\theta} = -2\pi\left(\int_0^\infty\int_0^\pi\zeta^5\cos\theta_\zeta\sin^3\theta_\zeta\Phi_s\mathrm{E}\,d\theta_\zeta\,d\zeta\right)\sin\theta, \tag{17h}$$

$$\mathrm{P}_{\varphi\varphi} = 3(\omega+\tau)-\mathrm{P}_{rr}-\mathrm{P}_{\theta\theta}, \qquad \mathrm{P}_{r\varphi}=\mathrm{P}_{\theta\varphi}=0, \tag{17i}$$

$$\mathrm{Q}_r = -\pi\left[\int_0^\infty\int_0^\pi\zeta^3(\zeta^2-\frac{5}{2})\sin 2\theta_\zeta\Phi_c\mathrm{E}\,d\theta_\zeta\,d\zeta\right]\cos\theta, \tag{17j}$$

$$\mathrm{Q}_\theta = \pi\left[\int_0^\infty\int_0^\pi\zeta^4(\zeta^2-\frac{5}{2})\sin^3\theta_\zeta\Phi_s\mathrm{E}\,d\theta_\zeta\,d\zeta\right]\sin\theta, \tag{17k}$$

$$\mathrm{Q}_\varphi = 0. \tag{17l}$$

IV. Outline of numerical analysis

We analyze the boundary-value problem for Φ_c and Φ_s in $[1 \le r < \infty, 0 \le \zeta < \infty, 0 \le \theta_\zeta \le \pi]$, given by Eqs. (9)–(12), numerically by the method developed in Ref. 12, which is basically an iterative finite-difference method and is described in detail there. Here we explain only the outline of the method and the points to be paid special attention to.

(i) In the numerical analysis we consider the problem in a finite domain ($1 \le r \le r_d$, $0 \le \zeta \le \zeta_d$, $0 \le \theta_\zeta \le \pi$) in (r, ζ, θ_ζ) space, where r_d and ζ_d are chosen properly depending on situations. Let $\widehat{\Phi}_s = \zeta \sin\theta_\zeta \Phi_s$, and $\widehat{\Phi} = \Phi_c$ and/or $\widehat{\Phi}_s$. We construct the discrete solution $\widehat{\Phi}_\#$ of $\widehat{\Phi}$ at the lattice points in (r, ζ, θ_ζ) space as the limit of the sequence $\widehat{\Phi}_\#^{(n)}$ obtained as follows. The initial solution $\widehat{\Phi}_\#^{(0)}$ is chosen properly. Let the solution $\widehat{\Phi}_\#^{(n)}$ be known. The solution $\widehat{\Phi}_\#^{(n+1)}$ for $0 \le \theta_\zeta < \pi/2$ is constructed from $r = r_d$ to $r = 1$ and then $\widehat{\Phi}_\#^{(n+1)}$ for $\pi/2 \le \theta_\zeta \le \pi$ from $r = 1$ to $r = r_d$ with the aid of Eqs. (9) and (10) discretized.

(ii) On the surface of the sphere, the velocity distribution function ϕ is discontinuous at $\zeta_i n_i = 0$ because the nature of the velocity distribution function of the incoming molecules ($\zeta_i n_i < 0$) and that of the outgoing molecules ($\zeta_i n_i > 0$) are different. The discontinuity propagates into the gas along the characteristic of Eq. (1) (*i.e.*, in the direction of ζ_i for which $\zeta_i n_i = 0$ on the boundary). Therefore, at a given point x_i in the gas, ϕ is discontinuous at ζ_i whose opposite vector $(-\zeta_i)$ lies on the circular cone along which the edge of the sphere is viewed from x_i (Fig. 2)[56]. In the present (r, ζ, θ_ζ) space, the discontinuity of $\widehat{\Phi}$ lies on the surface

$$r \sin\theta_\zeta = 1, \qquad (\pi/2 \le \theta_\zeta \le \pi). \tag{18}$$

The position of the discontinuity is independent of the molecular speed ζ. As the distance r increases, the discontinuity decays owing to molecular collisions.

When we discretize the equations for $\widehat{\Phi}$, which include derivative terms $\partial\widehat{\Phi}/\partial r$ and $\partial\widehat{\Phi}/\partial\theta_\zeta$, we should not apply finite-difference approximations for differentiation to these terms across the discontinuity. Therefore, we divide (r, ζ, θ_ζ) space into two regions by the discontinuity surface (18) and apply standard finite-difference approximations in each region. In this scheme, the limiting values of $\widehat{\Phi}_\#^{(n)}$ on the surface (18) from both sides are needed as the boundary condition. They are obtained separately by another finite-difference scheme along the characteristic (18). In the region where the discontinuity has decayed sufficiently, we use a standard finite-difference scheme for efficiency.

(iii) In the recursion formula to obtain $\widehat{\Phi}_\#^{(n+1)}$, the collision integrals for $\widehat{\Phi}$ [$\mathcal{L}_1^c(\Phi_c) - \mathcal{L}_2^c(\Phi_c)$ and $\mathcal{L}_1^s(\widehat{\Phi}_s) - \mathcal{L}_2^s(\widehat{\Phi}_s)$] are evaluated by the use of the data at the preceding step $\widehat{\Phi}_\#^{(n)}$. Since the collision integrals take the majority of the computing time of the whole analysis, their efficient computation is important. The computation of the collision integral $\mathcal{L}_1^c(\Phi_c) - \mathcal{L}_2^c(\Phi_c)$ or $\mathcal{L}_1^s(\widehat{\Phi}_s) - \mathcal{L}_2^s(\widehat{\Phi}_s)$ at the lattice point of (ζ, θ_ζ), say $(\zeta^{(i)}, \theta_\zeta^{(j)})$, is performed as follows[57]. The function $\widehat{\Phi}$ at the nth step is expanded in terms of a set of basis functions $\mathrm{B}_{kl}(\zeta, \theta_\zeta)$ as $\widehat{\Phi}(r, \zeta, \theta_\zeta) = \sum_{k,l} \widehat{\Phi}(r, \zeta^{(k)}, \theta_\zeta^{(l)}) \mathrm{B}_{kl}(\zeta, \theta_\zeta)$, where the set of basis functions $\mathrm{B}_{kl}(\zeta, \theta_\zeta)$ is chosen in such a way that $\widehat{\Phi}$ takes the exact value $\widehat{\Phi}(r, \zeta^{(k)}, \theta_\zeta^{(l)})$ at every lattice point $(\zeta^{(k)}, \theta_\zeta^{(l)})$ and is approximated by a continuous and sectionally quadratic function of ζ and θ_ζ. The set of the collision integrals of the basis functions forms a large matrix $\mathrm{M}_{(ij)(kl)}$ of (the number of the lattice points)$\times$(the number of the lattice points) (about 4400×4400 in the present work), where both of the double indices (ij) and (kl) can be put in a single index. Thus the collision integral $\mathcal{L}_1^c(\Phi_c) - \mathcal{L}_2^c(\Phi_c)$ or $\mathcal{L}_1^s(\widehat{\Phi}_s) - \mathcal{L}_2^s(\widehat{\Phi}_s)$ is expressed in the product of the matrix $\mathrm{M}_{(ij)(kl)}$ and the column vector $\widehat{\Phi}(r, \zeta^{(k)}, \theta_\zeta^{(l)})$ as $\sum_{k,l} \mathrm{M}_{(ij)(kl)} \widehat{\Phi}(r, \zeta^{(k)}, \theta_\zeta^{(l)})$. Since the two matrices, corresponding to $\mathcal{L}_1^c - \mathcal{L}_2^c$ and $\mathcal{L}_1^s - \mathcal{L}_2^s$, are universal constants (numerical

collision kernels), they can be computed beforehand and applied to other problems whose solutions are expressed by Eq. (7). Thus a very efficient computation of the collision integrals can be carried out. In the present computation, we use the numerical collision kernels constructed in Ref. 12.
(iv) The problem is considered in a finite domain ($1 \le r \le r_d$, $0 \le \zeta \le \zeta_d$, $0 \le \theta_\zeta \le \pi$) in (r, ζ, θ_ζ) space, where r_d and ζ_d are chosen properly depending on the situations. Because ϕE decays very rapidly as $\zeta \to \infty$, the truncation of ζ at $\zeta = \zeta_d$ of a moderate value does not cause any problem. The solution ϕ, however, approaches the value at infinity (12), say ϕ_∞, slowly as $r \to \infty$ ($\sim r^{-m}$). Therefore, a very large r_d is required to obtain an accurate result if the condition (12) is imposed directly at $r = r_d$. In order to avoid this difficulty, we match, at $r = r_d$, the numerical solution with the asymptotic solution for large r. For $r > r_A$ with large r_A, the effective length scale of variation of ϕ is $O(r_A L)$ [note that $\phi = O(r^{-m})$] and thus the effective Knudsen number $\ell_0/r_A L = Kn/r_A$ is small. Therefore, the asymptotic theory of the Boltzmann equation for small Knudsen numbers[1,2,4,5] can be used to obtain the asymptotic solution for large r.
(v) For small Knudsen numbers, molecular collisions [or the collision term of Eq. (1)] play the dominant role in the behavior of the gas [or Eq. (1)]. Thus, a small error of computation of the collision integral of Eq. (1) is magnified in the solution. It is very inefficient (and unpractical in the present situation) to carry out more detailed computation than that carried out in Ref. 12. We can, however, bypass the difficulty by making use of the asymptotic theory[1,2,4,56,5] of the general boundary-value problem of the Boltzmann equation for small Knudsen numbers. Let $\phi_{A[N]}$ be the asymptotic solution of the problem:

$$\phi = \phi_{A[N]} + O(k^{N+1}). \tag{19}$$

The $\phi_{A[N]}$ is expressed by the sum of the global solution $\phi_{G[N]}$ (hydrodynamic part) and its local correction $\phi_{K[N]}$ (Knudsen-layer and S-layer correction) near the sphere. Put ϕ as

$$\phi = \phi_{G[1]} + \tilde{\phi}, \tag{20}$$

then $\tilde{\phi}$ is determined by

$$\zeta_i \frac{\partial \tilde{\phi}}{\partial x_i} = \frac{1}{k} \mathcal{L}(\tilde{\phi}) - \zeta_i \frac{\partial (\phi_{G[1]} - \phi_{G[0]})}{\partial x_i}, \tag{21}$$

where the relation $\mathcal{L}(\phi_{G[1]}) = k\zeta_i \partial \phi_{G[0]}/\partial x_i$ (*see* Refs. 1, 4, and 5) was used. Then, $\tilde{\phi} = O(k^2)$ outside the Knudsen layer and $\tilde{\phi} = O(k)$ in the Knudsen layer since $\phi_{G[0]} = \phi_{A[0]}$ in the present problem. Equation (21) is, theoretically, equivalent to Eq. (1), but is appropriate for numerical computation for small k, since the relative error of $\tilde{\phi}$ obtained by Eq. (21) for rigorous or very precise $\phi_{G[1]} - \phi_{G[0]}$ is of the same order of that of ϕ obtained by Eq. (1).

V. Flow field and force on the sphere

A. Numerical solution

The numerical computation was, in most cases, carried out with the same lattice system that was used in Ref. 12. Some small improvements, as well as the method (v) in the previous section, were introduced where some difficulty to maintain the accuracy arises in the straightforward computation. The numerical solutions are supplemented by the analytical solutions for two extreme cases: small and infinite Knudsen numbers in Sec. B.

The macroscopic variables obtained from Φ_c and Φ_s by Eqs. (17a)–(17l) have simple θ dependence; that is, $\omega/\cos\theta$, $\tau/\cos\theta$, $u_r/\cos\theta$, $u_\theta/\sin\theta$, etc. are functions of r only. The distributions of $\omega/\alpha\cos\theta$, $\tau/\alpha\cos\theta$, $u_r/\alpha\cos\theta$, and $u_\theta/\alpha\sin\theta$ are shown in Figs. 3(a)–4(b) for various k, where the free molecular solution and the Stokes solution without slip are also shown. The effect of the sphere with the nonuniform temperature on the density and temperature fields is larger and extends

in a wider range for smaller Knudsen numbers. A flow is induced around a sphere in the positive x_1 direction for $\alpha > 0$, as a whole, irrespective of k. The flow vanishes at the two limiting cases ($k = 0$ and ∞) [*cf.* Eqs. (27c), (30a), and (30b)], and reaches the maximum at $k = 0.2 \sim 0.4$. The streamlines of the flow are shown for $k = 0.05$, 0.2, 1, and 2 in Figs. 5(a)–5(d), where the arrows show the direction of the flow for $\alpha > 0$. The flow speeds near the sphere (or maximum speeds) for $k = 0.05$ and 1 are fairly close, but the decay with the distance from the sphere is faster for $k = 0.05$ [Figs. 4(a) and 4(b); compare Fig. 5(a) with Fig. 5(c)]. The flow velocity in the far field is proportional to $1/r$ commonly to k; the constant of proportion, however, depends on k. The heat flow $Q_r/\alpha \cos\theta$ at $r = 1$, which is important to derive the drag and thermal force of a spherical particle with an arbitrary thermal conductivity, is shown in Fig. 6. It vanishes at $k = 0$ [Eq. (31)], increases monotonically as k increases, and reaches $1/\sqrt{\pi}$ at $k = \infty$ [Eq. (28b)].

The force F_i acting on the sphere is expressed as

$$F_1 = p_0 L^2 \alpha h(k), \tag{22a}$$

$$F_2 = F_3 = 0, \tag{22b}$$

where h is given in Fig. 7 and Table I. The h is zero at $k = 0$ [Eq. (32)], decreases monotonically as k increases, and reaches $-\pi/3$ at $k = \infty$ [Eq. (29)]. Thus, the force is in the negative x_1 direction for $\alpha > 0$; that is, the force is in the opposite direction to that of the overall flow. It is noted that the sphere is subject to a force at $k = \infty$ although there is no flow. This is a typical feature of a free molecular gas[58–60,5]. (In the continuum gas or the Navier-Stokes gas without external forces, no flow corresponds to no force on a closed body.)

In the free molecular flow, the velocity distribution function of the molecules impinging on a small surface element dS on the sphere is the corresponding part of the distribution at infinity. The mass flux and the magnitude of the momentum flux due to the molecules impinging on dS, therefore, are uniform over the sphere; the direction of the momentum flux is normal to dS. Thus, the total momentum flux to the sphere due to the impinging molecules vanishes. The mass flux due to the molecules outgoing from dS is also uniform over the sphere, since there is no evaporation or condensation on the sphere. On the other hand, the molecules outgoing from the hotter side of the sphere have higher speed on the average; correspondingly the magnitude of the momentum flux due to the outgoing molecules is larger on the hotter side, because of the uniform mass flux. The total momentum flux leaving the sphere, therefore, is in the direction to the hotter from the colder side of the sphere. Thus, the net momentum flux to the sphere of all the molecules (impinging and outgoing) and, therefore, the force on the sphere are in the direction to the colder from the hotter side of the sphere, *i.e.*, in the negative x_1 direction for $\alpha > 0$. (In this situation the mass flux vanishes everywhere in the gas as well as on the sphere, although this is not intuitively obvious[58,59].) Molecular collisions transfer the momentum flux of the outgoing molecules from the sphere, which is totally in the x_1 direction for $\alpha > 0$ and escapes to infinity in the free molecular case, to surrounding gas molecules. Thus, a flow is induced, and the force on the sphere is decreased.

The cause of the flow can be understood locally as follows. Consider the momentum transferred to dS from the gas. Here the component of the momentum tangential (or parallel) to dS is of our interest. Then we only have to estimate the momentum flux due to the molecules impinging on dS, since the momentum flux due to the molecules outgoing from dS has no tangential component in the case of the diffuse reflection. In the free molecular gas, the momentum flux due to the impinging molecules, which is not affected by the sphere, does not have any tangential component. For finite Knudsen numbers, the velocity distribution around the sphere, of the molecules directing toward the sphere is also affected by the sphere. The molecules impinging on dS come directly (or without collision with other molecules) from a region about a mean free path away from dS. Thus, the molecules impinging on dS from the hotter (colder) side have higher (lower) speed on the average. The momentum flux due to the impinging molecules, therefore, has a tangential

component toward the colder side. Thus, the surface element dS is subject to a force toward the colder side along dS. The gas is subject to its reaction, and a steady flow is induced in such a way that the momentum flux due to the flow induced counterbalances the original momentum flux (the thermal creep effect[6–8]). The flow speed increases as the Knudsen number decreases, since more impinging molecules are accelerated or decelerated by molecular collisions. If the Knudsen number becomes very small, however, the molecules proceed only a very short distance before the next collision, and the velocity distribution function becomes isotropic. Thus the tangential momentum flux vanishes and no flow is induced in the continuum limit. The flow, therefore, has its maximum at some intermediate Knudsen number.

The force on the sphere can be computed by integrating the momentum flux over any control surface enclosing the sphere. In principle this serves a good accuracy test of computation, but in practice it is too severe a test to be applied to a large control surface, where the force is obtained as a small quantity integrated over a large area. Small errors in local variables are multiplied by the factor r_c^2, where r_c is the characteristic dimension of the control surface, and lead to a considerable error in the force. The data in Table I are computed on the sphere. For a test of the accuracy of the computation, the variation (max − min) of h computed on the control spheres $r = r^{(i)}$ for all the lattice points $r^{(i)}$ between $r = 1$ and 4 is also shown in Table I.

The Φ_c and Φ_s at $\zeta = 0.556$ over $r\,\theta_\zeta$ plane are shown in Figs. 8(a)–11(b). The surfaces Φ_c and Φ_s are separated by their discontinuities at $r\sin\theta_\zeta = 1$ $(\pi/2 \le \theta_\zeta \le \pi)$ [*cf.* Sec. IV(ii)]. The discontinuity is the border of the region $[\pi - \mathrm{Arcsin}(1/r) \le \theta_\zeta \le \pi]$, say region I, that can be reached directly by a molecule from the sphere. In the free molecular flow ($k = \infty$), whose analytical solution is given in Sec. B, the velocity distribution function ϕ is constant along a characteristic of Eq. (1) and it is equal to the value at the starting point of the characteristic (the sphere or infinity). Thus ϕ (and therefore Φ_c and Φ_s) is zero in the region $[0 \le \theta_\zeta < \pi - \mathrm{Arcsin}(1/r)]$, say region II. The size of the discontinuity of ϕ is invariant along the discontinuity ($r\sin\theta_\zeta = 1$), but that of Φ_c or Φ_s should be noted to vary along $r\sin\theta_\zeta = 1$ [Figs. 8(a) and 8(b)]. For a finite value of k, ϕ on different characteristics interacts by molecular collisions, and Φ_c and Φ_s deviate from the free molecular ones in Figs. 8(a) and 8(b). At $k = 10$, Φ_c and Φ_s are little affected by molecular collisions in region II, but they are affected considerably some distance away from the sphere in region I [Figs. 9(a) and 9(b)]. The discontinuity decays in several mean free paths ($r = 20 \sim 30$) from the sphere. At $k = 1$, the effect of molecular collisions is appreciable over all r in region I and within some distance from the sphere in region II [Figs. 10(a) and 10(b)]. It is stronger near the discontinuity. The discontinuity also decays in several mean free paths ($r = 2 \sim 3$) from the sphere. The overall feature is similar to that of the case $k = 10$. At $k = 0.1$, the overall feature is considerably different; the effect of collision prevails over the whole region [Figs. 11(a) and 11(b)]. The discontinuity decays in a much shorter distance than the mean free path. As explained in Ref. 56, the discontinuity decays in several (mean) free paths along the characteristic $r\sin\theta_\zeta = 1$, but the distance from the sphere to the part of the characteristic where discontinuity is appreciable is much smaller than the mean free path, because the characteristic is still nearly parallel to the surface of the sphere for several mean free paths in the case of small Knudsen numbers (*cf.* Fig. 7 in Ref. 56). After the discontinuity disappears, Φ_c and Φ_s are further deformed and become smoother in a few mean free paths ($r = 1.2 \sim 1.3$) from the sphere. Further away from the sphere their deformation is roughly expressed with a global scale change (similar deformation) and they vanish at infinity. The region with discontinuity is the S layer[61,56] at the bottom of the Knudsen layer, the intermediate region is the Knudsen layer, and the outer region is the hydrodynamic region[1,2,4,5]. Figures 8(a)–11(b) show Φ_c and Φ_s for a representative molecular speed ($\zeta = 0.556$). For smaller (or larger) molecular speed, the free path of the molecule is smaller (or larger), and therefore the behavior of Φ_c and Φ_s shows the feature of smaller (or larger) Knudsen number. The surfaces Φ_c and Φ_s for $k = 1$ at $\zeta = 0.139$ and those for $k = 1$ at $\zeta = 1.70$ are shown in Figs. 12(a)–13(b).

We have also computed the same problem on the basis of the BKW (Boltzmann-Krook-Welander

or BGK) equation[62–64] by the same finite-difference method. Some of the results are shown in Figs. 6 and 7 for comparison. The way of comparing the results of different molecular models is not unique. The present problem contains two parameters α and k. The parameter k can be replaced by $\mu_g/\rho_0 \mathrm{L}(\mathrm{RT}_0)^{1/2}$, $\lambda_g(\mathrm{RT}_0)^{1/2}/p_0\mathrm{LR}$, or $(\mu_g\lambda_g)^{1/2}\mathrm{T}_0^{1/2}/p_0\mathrm{L}$, where μ_g and λ_g are, respectively, the viscosity and thermal conductivity of the gas at the reference state, since μ_g and λ_g are related to ℓ_0 as $\mu_g = (\sqrt{\pi}/2)\gamma_1 p_0(2\mathrm{RT}_0)^{-1/2}\ell_0$ and $\lambda_g = (5/4)\sqrt{\pi}\gamma_2 p_0(2\mathrm{RT}_0)^{-1/2}\mathrm{R}\ell_0$, where $\gamma_1 = 1.270042$ and $\gamma_2 = 1.922284$ for the hard-sphere molecular gas, and $\gamma_1 = \gamma_2 = 1$ for the BKW model.[4,10] The result of comparison, however, depends on the choice of the parameter, because the relation between ℓ_0 and μ_g, λ_g, or $(\mu_g\lambda_g)^{1/2}$ differs by molecular models. When $\mu_g/\rho_0\mathrm{L}(\mathrm{RT}_0)^{1/2}$ (or μ_g) is taken as the basic parameter instead of k (or ℓ_0), k for the BKW model is related to k for the hard-sphere molecular gas as

$$k\ (\mathrm{BKW}) = 1.270042k\ (\text{hard sphere}). \tag{23}$$

With $\lambda_g(\mathrm{RT}_0)^{1/2}/p_0\mathrm{LR}$ (or λ_g) as the basic parameter,

$$k\ (\mathrm{BKW}) = 1.922284k\ (\text{hard sphere})\ . \tag{24}$$

With $(\mu_g\lambda_g)^{1/2}\mathrm{T}_0^{1/2}/p_0\mathrm{L}$ [or $(\mu_g\lambda_g)^{1/2}$] as the basic parameter,

$$k\ (\mathrm{BKW}) = 1.562492k\ (\text{hard sphere})\ . \tag{25}$$

In Fig. 6 (7) the conversion (25) [(24)] is used to show the BKW result.

The computation was carried out on HP 9000 730 computers at our laboratory (for the BKW equation) and FUJITSU VP-2600 computer at the Data Processing Center of Kyoto University (for the Boltzmann equation for hard-sphere molecules).

B. Free molecular solution and asymptotic solution for small Knudsen numbers

Here, we summarize the analytical solutions for two extreme cases: the free molecular solution and the asymptotic solution for small Knudsen numbers. The free molecular solution can be easily obtained as follows:

$$\frac{\Phi_c}{\alpha} = \begin{cases} 0, & [0 \le \theta_\zeta < \pi - \mathrm{Arcsin}(1/r)], \\ (\zeta^2-2)[r\sin^2\theta_\zeta - \cos\theta_\zeta(1 - r^2\sin^2\theta_\zeta)^{1/2}], & \\ & [\pi - \mathrm{Arcsin}(1/r) \le \theta_\zeta \le \pi], \end{cases} \tag{26a}$$

$$\frac{\Phi_s}{\alpha} = \begin{cases} 0, & [0 \le \theta_\zeta < \pi - \mathrm{Arcsin}(1/r)], \\ -\zeta^{-1}(\zeta^2-2)[r\cos\theta_\zeta + (1 - r^2\sin^2\theta_\zeta)^{1/2}], & \\ & [\pi - \mathrm{Arcsin}(1/r) \le \theta_\zeta \le \pi], \end{cases} \tag{26b}$$

$$\frac{\omega}{\alpha\cos\theta} = -\frac{1}{12}[2r - (2+r^{-2})(1-r^{-2})^{1/2}r + r^{-2}], \tag{27a}$$

$$\frac{\tau}{\alpha\cos\theta} = \frac{1}{6}[2r - (2+r^{-2})(1-r^{-2})^{1/2}r + r^{-2}], \tag{27b}$$

$$\frac{u_r}{\alpha\cos\theta} = \frac{u_\theta}{\alpha\sin\theta} = 0, \tag{27c}$$

$$\frac{Q_r}{\alpha\cos\theta} = \frac{1}{2\sqrt{\pi}}[r^{-3} + 4r^{-2}\int_0^1 y(1-y^2)^{1/2}(1-y^2/r^2)^{1/2}dy], \tag{28a}$$

especially, at $r = 1$

$$\frac{Q_r}{\alpha \cos\theta} = \frac{1}{\sqrt{\pi}}, \tag{28b}$$

$$h = -\frac{\pi}{3}. \tag{29}$$

No flow is induced in the free molecular case, which is proved under a more general condition in Refs. 58 and 59. Various examples of forces on heated bodies in a free molecular gas at rest are given in Refs. 60, 65, and 5.

The asymptotic solution for small Knudsen numbers can also be easily obtained with the aid of the asymptotic theory[1,2,4,56,5] of the boundary value problem of the Boltzmann equation as follows:

$$\frac{u_r}{\alpha \cos\theta} = \mathrm{K}_1 k(-r^{-1} + r^{-3}), \tag{30a}$$

$$\frac{u_\theta}{\alpha \sin\theta} = \frac{1}{2}\mathrm{K}_1 k(r^{-1} + r^{-3}) + \frac{1}{2}k\mathrm{Y}_1(\eta), \tag{30b}$$

$$\frac{\omega}{\alpha \cos\theta} = -(1 - 2d_1 k)r^{-2} - 2k\Omega_1(\eta), \tag{30c}$$

$$\frac{\tau}{\alpha \cos\theta} = (1 - 2d_1 k)r^{-2} - 2k\Theta_1(\eta), \tag{30d}$$

$$\frac{Q_r}{\alpha \cos\theta} = \frac{5}{2}\gamma_2(1 - 2d_1 k)kr^{-3} - 2k^2 \int_\eta^\infty \mathrm{H_B}(y)dy, \tag{31}$$

$$h = 4\pi\gamma_1 \mathrm{K}_1 k^2, \tag{32}$$

where d_1 and K_1 are, respectively, the temperature jump and thermal creep slip coefficients $\{d_1 = 2.4001$, $\mathrm{K}_1 = -0.6463$ (hard sphere); $d_1 = 1.30272$, $\mathrm{K}_1 = -0.38316$ (BKW) (Refs. 8 and 57) [d_1 (here) $= \beta$ (Ref. 57) and K_1 (here) $= -\beta_\mathrm{B}$ (Ref. 8)]$\}$; $\Theta_1(\eta)$, $\Omega_1(\eta)$, $\mathrm{Y}_1(\eta)$, and $\mathrm{H_B}(\eta)$, called the Knudsen-layer functions, are functions of the stretched coordinate η defined $\eta = (r - 1)/k$ and tabulated in Refs. 8 and 57 $\{[\Theta_1(\eta), \Omega_1(\eta), \mathrm{H_B}(\eta), \eta]$ (here, Ref. 4) $= [\Theta(x_1), \Omega(x_1), \mathrm{H_B}(x_1), x_1]$ (Ref. 8) and $[\mathrm{Y}_1(\eta), \eta]$ (here, Ref. 4) $= [-2\mathrm{C}(x_1), x_1]$ (Ref. 57)$\}$. Equations (30a)–(30d) are correct up to the order of k, and Eqs. (31) and (32) up to the order of k^2.

VI. Drag and thermal force problems of a spherical particle with an arbitrary thermal conductivity

In this section the drag and thermal force problems of a spherical particle with an arbitrary thermal conductivity are considered. The drag problem (Problem D) is concerned with a particle placed in a uniform flow [velocity: $\mathrm{U}_{\infty i} = ((2\mathrm{RT}_0)^{1/2}u_\infty, 0, 0)$, pressure: p_0, temperature: T_0] of a gas, and the thermal force problem (Problem T) is concerned with a particle placed in a gas at rest with a small uniform temperature gradient [pressure: p_0, temperature: $\mathrm{T} = \mathrm{T}_0(1 + \beta x_1)$, temperature gradient: $(\partial \mathrm{T}/\partial \mathrm{X}_i)_\infty = (\beta \mathrm{T}/\mathrm{L}, 0, 0)$]. These problems for a spherical particle with a uniform surface temperature (or a spherical particle with a very large thermal conductivity) are studied in Refs. 12 and 47. We will show that the solution of Problem D or T for the general case (arbitrary thermal conductivity) can be constructed with that of Problem D or T for the special case (infinite thermal conductivity) and that of the problem studied in Secs. III–V. In the following analysis the same nondimensional variables as those introduced in Sec. II are used with the additional subscript D or T to indicate Problem D or T. The only exception is the nondimensional force h on the particle for which h, h_D, and h_T are nondimensionalized by different quantities, *i.e.*, by $p_0\mathrm{L}^2\alpha$, $p_0\mathrm{L}^2\mathrm{U}_{\infty i}(2\mathrm{RT}_0)^{-1/2}$, and $\mathrm{L}^2\lambda_g(\partial \mathrm{T}/\partial \mathrm{X}_i)_\infty(2\mathrm{RT}_0)^{-1/2}$, respectively.

In the problems for a particle with a finite value of the thermal conductivity, the flow field of the gas and the temperature field inside the particle $[\mathrm{T}_p = \mathrm{T}_0(1 + \tau_p)]$ are interrelated. They have

to be analyzed simultaneously. The problems are given by the following systems. The behavior of the gas is described by Eq. (1):

$$\zeta_i \frac{\partial \phi_{\mathrm{DT}}}{\partial x_i} = \frac{1}{k}\mathcal{L}(\phi_{\mathrm{DT}}), \qquad (\mathrm{DT} = \mathrm{D\ or\ T}).$$

The temperature τ_p inside the particle is governed by the Laplace equation:

$$\frac{\partial^2 \tau_p}{\partial x_i^2} = 0. \tag{33}$$

On the surface S of the particle, in addition to the diffuse reflection condition:

$$\phi_{\mathrm{DT}}(x_i \in \mathrm{S}, \zeta_i) = (\zeta^2 - 2)\tau_p|_{\mathrm{S}} - 2\pi^{1/2} \int_{\zeta_i n_i < 0} \zeta_j n_j \phi_{\mathrm{DT}} \mathrm{E}\, d\zeta_1\, d\zeta_2\, d\zeta_3, \quad (\zeta_i n_i > 0), \tag{34}$$

the condition of continuity of the energy flux through the surface S is required:

$$\left.\frac{\partial \tau_p}{\partial x_i}\right|_{\mathrm{S}} n_i = -\frac{4}{5} k^{-1} \gamma_2^{-1} \frac{\lambda_g}{\lambda_p}\, \mathrm{Q}_{i\mathrm{DT}}|_{\mathrm{S}}\, n_i, \tag{35}$$

where λ_p is the thermal conductivity of the particle. The condition at infinity, which is the same as that in Ref. 12 or 47, is given

$$\phi_{\mathrm{DT}} \to \phi_{\mathrm{DT}\infty}, \tag{36}$$

where

$$\phi_{\mathrm{D}\infty} = 2\zeta_1 u_\infty, \tag{37}$$

$$\phi_{\mathrm{T}\infty} = \beta[(\zeta^2 - \frac{5}{2})x_1 - k\zeta_1 \mathrm{A}(\zeta)], \tag{38}$$

where $\mathrm{A}(\zeta)$ is the solution of the following integral equation[66,10]:

$$\begin{cases} \mathcal{L}[\zeta_i \mathrm{A}(\zeta)] = -\zeta_i(\zeta^2 - \frac{5}{2}), \\ \quad \text{subsidiary condition:} \\ \quad \displaystyle\int_0^\infty \zeta^4 \mathrm{A}(\zeta) \exp(-\zeta^2) d\zeta = 0. \end{cases} \tag{39}$$

We put

$$\phi_{\mathrm{DT}} = \phi_{\mathrm{I}} + \phi_{\mathrm{DT}}(\lambda_p = \infty), \tag{40}$$

where $\phi_{\mathrm{DT}}(\lambda_p = \infty)$ is the solution ϕ_{DT} for the particle with a uniform temperature or $\lambda_p = \infty$. The first term ϕ_{I} on the right hand side in Eq. (40), dependent on D or T, is denoted by $\phi_{\mathrm{I(DT)}}$ when discrimination is required. Then, ϕ_{I} satisfies the same equation as ϕ_{DT} or Eq. (1):

$$\zeta_i \frac{\partial \phi_{\mathrm{I}}}{\partial x_i} = \frac{1}{k}\mathcal{L}(\phi_{\mathrm{I}}). \tag{41}$$

The diffuse reflection condition (34) is reduced to

$$\phi_{\mathrm{I}}(x_i \in \mathrm{S}, \zeta_i) = (\zeta^2 - 2)\tau_p|_{\mathrm{S}} - 2\pi^{1/2} \int_{\zeta_i n_i < 0} \zeta_j n_j \phi_{\mathrm{I}} \mathrm{E}\, d\zeta_1\, d\zeta_2\, d\zeta_3, \quad (\zeta_i n_i > 0), \tag{42}$$

and the condition of continuity of the energy flux (35) is

$$\left.\frac{\partial \tau_p}{\partial x_i}\right|_{\mathrm{S}} n_i = -\frac{4}{5} k^{-1} \gamma_2^{-1} \frac{\lambda_g}{\lambda_p} [\mathrm{Q}_{i\mathrm{I}} + \mathrm{Q}_{i\mathrm{DT}}(\lambda_p = \infty)]_{\mathrm{S}}\, n_i. \tag{43}$$

The condition at infinity is simply

$$\phi_{\mathrm{I}} \to 0. \tag{44}$$

The problems become simple for a spherical particle. Noting that $\tau_p = \alpha_{\mathrm{I}} r \cos\theta$ [α_{I} is also denoted by $\alpha_{\mathrm{I(DT)}}$ for discrimination] is a solution of Eq. (33), we find that ϕ_{I} in the form of Eq. (7), *i.e.*,

$$\phi_{\mathrm{I}} = \Phi_{c\mathrm{I}}(r, \zeta, \theta_\zeta)\cos\theta + \zeta_\theta \Phi_{s\mathrm{I}}(r, \zeta, \theta_\zeta)\sin\theta, \tag{45}$$

is consistent with the boundary conditions as well as Eq. (41). That is, $\Phi_{c\mathrm{I}}$ and $\Phi_{s\mathrm{I}}$ are governed by Eqs. (9) and (10) (with $\Phi_c = \Phi_{c\mathrm{I}}$ and $\Phi_s = \Phi_{s\mathrm{I}}$). Corresponding to Eqs. (42) and (43),

$$\begin{cases} \Phi_{c\mathrm{I}} = (\zeta^2 - 2)\alpha_{\mathrm{I}} + 2\pi^{3/2} \displaystyle\int_0^\infty \int_0^{\pi/2} \zeta^3 \sin 2\theta_\zeta \Phi_{c\mathrm{I}} \mathrm{E}\, d\theta_\zeta\, d\zeta, & (\pi/2 \le \theta_\zeta \le \pi), \\ \Phi_{s\mathrm{I}} = 0, \end{cases} \tag{46}$$

and

$$\mathrm{Q}_{r\mathrm{I}}|_{r=1} = -\mathrm{Q}_{r\mathrm{DT}}(\lambda_p = \infty)|_{r=1} - \frac{5}{4} k \gamma_2 \frac{\lambda_p}{\lambda_g} \alpha_{\mathrm{I}} \cos\theta. \tag{47}$$

From Eq. (44), the condition at infinity is

$$\Phi_{c\mathrm{I}} \to 0, \quad \Phi_{s\mathrm{I}} \to 0. \tag{48}$$

The solution of Eqs. (9) and (10), with $\Phi_c = \Phi_{c\mathrm{I}}$ and $\Phi_s = \Phi_{s\mathrm{I}}$, under the boundary conditions (46) and (48), with undetermined α_{I}, is given in terms of Φ_c and Φ_s in Secs. III–V as

$$(\Phi_{c\mathrm{I}}, \Phi_{s\mathrm{I}}) = \frac{\alpha_{\mathrm{I}}}{\alpha}(\Phi_c, \Phi_s), \tag{49}$$

[*cf.* Eqs. (11) and (12)]. In other words the solution is obtained by replacing α in the solution in Secs. III–V by α_{I}. Thus $\mathrm{Q}_{r\mathrm{I}}$ is given by $(\alpha_{\mathrm{I}}/\alpha)\mathrm{Q}_r$ with Q_r in Secs. III–V. Substituting this $\mathrm{Q}_{r\mathrm{I}}|_{r=1}$ in Eq. (47), we obtain the constant α_{I} as

$$\alpha_{\mathrm{I}} = \left. \frac{-(4/5)k^{-1}\gamma_2^{-1}(\lambda_g/\lambda_p)[\mathrm{Q}_{r\mathrm{DT}}(\lambda_p = \infty)/\cos\theta]}{1 + (4/5)k^{-1}\gamma_2^{-1}(\lambda_g/\lambda_p)(\mathrm{Q}_r/\alpha\cos\theta)} \right|_{r=1}, \tag{50}$$

It is noted here that $\mathrm{Q}_{r\mathrm{D}}(\lambda_p = \infty)/u_\infty \cos\theta$, $\mathrm{Q}_{r\mathrm{T}}(\lambda_p = \infty)/\beta\cos\theta$, and $\mathrm{Q}_r/\alpha\cos\theta$ at $r = 1$ are functions of k only.

Thus, the solution of the drag or thermal force problem for a spherical particle with an arbitrary thermal conductivity is given by the sum [Eq. (40)] of the corresponding solution for the particle with $\lambda_p = \infty$ and the solution in Secs. III–V with $\alpha = \alpha_{\mathrm{I}}$. Therefore the drag $\mathrm{F}_{\mathrm{D}i}$ and the thermal force $\mathrm{F}_{\mathrm{T}i}$ are given by

$$\mathrm{F}_{\mathrm{D}i} = p_0 \mathrm{L}^2 \mathrm{U}_{\infty i} (2\mathrm{RT}_0)^{-1/2} h_{\mathrm{D}}, \tag{51a}$$

$$h_{\mathrm{D}} = h_{\mathrm{D}}(\lambda_p = \infty) + \frac{\alpha_{\mathrm{I(D)}}}{u_\infty} h, \tag{51b}$$

with

$$\frac{\alpha_{\mathrm{I(D)}}}{u_\infty} = \left. \frac{-(4/5)k^{-1}\gamma_2^{-1}(\lambda_g/\lambda_p)[\mathrm{Q}_{r\mathrm{D}}(\lambda_p = \infty)/u_\infty \cos\theta]}{1 + (4/5)k^{-1}\gamma_2^{-1}(\lambda_g/\lambda_p)(\mathrm{Q}_r/\alpha\cos\theta)} \right|_{r=1}, \tag{51c}$$

and

$$\mathrm{F}_{\mathrm{T}i} = (2\mathrm{RT}_0)^{-1/2} \mathrm{L}^2 \lambda_g \left(\frac{\partial \mathrm{T}}{\partial \mathrm{X}_i} \right)_\infty h_{\mathrm{T}}, \tag{52a}$$

$$h_{\mathrm{T}} = h_{\mathrm{T}}(\lambda_p = \infty) + \frac{4}{5} k^{-1} \gamma_2^{-1} \frac{\alpha_{\mathrm{I(T)}}}{\beta} h, \tag{52b}$$

with

$$\frac{\alpha_{\mathrm{I(T)}}}{\beta} = \left.\frac{-(\lambda_g/\lambda_p)[\mathrm{Q}_{r\mathrm{T}}(\lambda_p=\infty)/(5/4)k\gamma_2\beta\cos\theta]}{1+(4/5)k^{-1}\gamma_2^{-1}(\lambda_g/\lambda_p)(\mathrm{Q}_r/\alpha\cos\theta)}\right|_{r=1}. \tag{52c}$$

Here, h_{D} and h_{T} are functions of k and λ_p/λ_g; the flow velocity $\mathrm{U}_{\infty i}$ in Eq. (51a) and the temperature gradient $(\partial \mathrm{T}/\partial \mathrm{X}_i)_\infty$ in Eq. (52a) do not have to be in the X_1 direction. The necessary information to obtain h_{D} and h_{T}, *i.e.*, $h_{\mathrm{D}}(\lambda_p=\infty)$, $h_{\mathrm{T}}(\lambda_p=\infty)$, $\mathrm{Q}_{r\mathrm{D}}(\lambda_p=\infty)|_{r=1}/u_\infty\cos\theta$, $\mathrm{Q}_{r\mathrm{T}}(\lambda_p=\infty)|_{r=1}/(5/4)k\gamma_2\beta\cos\theta$, h, and $\mathrm{Q}_r|_{r=1}/\alpha\cos\theta$, is given in Table II. (The nondimensional forces $h_{\mathrm{D}}(\lambda_p=\infty)$ and $h_{\mathrm{T}}(\lambda_p=\infty)$ are, respectively, denoted by h_{D} in Ref. 12 and h_{T} in Ref. 47. The third and fourth quantities, related to Refs. 12 and 47 as well as the first and second, are not shown in these papers.) The asymptotic form of h_{D} and h_{T} for large and small k are as follows: The leading terms of h_{D} and h_{T} for large k are

$$h_{\mathrm{D}} = h_{\mathrm{D}}(\lambda_p=\infty) = \frac{2}{3}\sqrt{\pi}(\pi+8), \tag{53}$$

$$h_{\mathrm{T}} = h_{\mathrm{T}}(\lambda_p=\infty) = -\frac{32\sqrt{\pi}}{15}\gamma_2^{-1}\int_0^\infty \zeta^5\mathrm{A}(\zeta)\exp(-\zeta^2)d\zeta, \tag{54}$$

which are independent of λ_p/λ_g. The h_{D}, up to $\mathrm{O}(k^2)$, and h_{T}, up to $\mathrm{O}(k)$, for small k are

$$h_{\mathrm{D}} = h_{\mathrm{D}}(\lambda_p=\infty) = 6\pi\gamma_1 k(1+k_0 k), \tag{55}$$

$$h_{\mathrm{T}} = \frac{16\pi}{5}\frac{3\lambda_g/\lambda_p}{1+2\lambda_g/\lambda_p}\gamma_1\gamma_2^{-1}\mathrm{K}_1 k, \tag{56}$$

where k_0 is the shear slip coefficient [$k_0 = -1.2540$ (hard sphere), $= -1.01619$ (BKW); k_0 (here) $= -\beta_{\mathrm{A}}$ (Ref. 8)]. The drag h_{D} is independent of λ_p/λ_g up to the order of k^2.

The profile h_{D} vs k and h_{T} vs k are shown for several λ_p/λ_g in Figs. 14 and 15 respectively. In these figures, the asymptotic solutions for large and small k are also shown. Experimental results of the thermal force by several authors, which range from $k \cong 0.047$ to 3.2, are also shown in Fig. 15. The numerical and experimental results, except the data in Ref. 32, agree well, especially for small Knudsen numbers. The drag h_{D} depends little on λ_p/λ_g, but the thermal force h_{T} depends considerably on λ_p/λ_g. The numerical and experimental results, which are limited to $k \gtrsim 0.05$, do not show negative thermophoresis (Fig. 15). The asymptotic solution for very large λ_p/λ_g and small k shows negative thermophoresis. The corresponding numerical result is very small, and the transition to the asymptotic solution seems to be smooth. Judging from the asymptotic solution at $k = 0.01$, the negative thermophoresis can be observed for a particle with $\lambda_p/\lambda_g \gtrsim 2\times 10^3$. Loyalka's numerical results for $k \cong 0.52$ to 5.2 and $\lambda_p/\lambda_g = 10$ and 100 in Ref. 45 based on his model equation are also shown in Fig. 15. The model equation is derived by replacing the kernel of the collision integral of the Boltzmann equation by the first few terms of the associated Legendre function expansion of the exact kernel. The truncated kernel of the first four term expansion adopted in Ref. 45 is considerably different from the exact kernel[67]; that is, the equation derived is considerably different from the original linearized Boltzmann equation for hard-sphere molecules. The force obtained, however, is fairly close to the present result.

If the spherical particle is left in the gas at rest with a uniform temperature gradient, it begins to move owing to the force (52a). To estimate its final velocity, we consider the particle in a uniform flow of a gas with a uniform temperature gradient [flow velocity $\mathrm{U}_{\infty i}$, pressure p_0, and temperature $\mathrm{T}_0 + (\partial \mathrm{T}/\partial \mathrm{X}_i)_\infty \mathrm{X}_i$]. Then, the force acting on the particle is the sum of Eqs. (51a) and (52a). Therefore, the force vanishes if the relative velocity of the particle V_i to the uniform flow $\mathrm{U}_{\infty i}$ is

$$\mathrm{V}_i = -\mathrm{U}_{\infty i} = \lambda_g p_0^{-1}\left(\frac{\partial \mathrm{T}}{\partial \mathrm{X}_i}\right)_\infty \frac{h_{\mathrm{T}}}{h_{\mathrm{D}}}. \tag{57}$$

The situation considered does not exactly correspond to the original one, where the particle is moving in a stationary gas with a temperature gradient. In the latter case, in the frame fixed to the particle, the particle lies in the gas with velocity $-\mathrm{V}_i$, pressure p_0, and temperature $\mathrm{T}_0 + (\partial \mathrm{T}/\partial \mathrm{X}_i)_\infty(\mathrm{X}_i + \mathrm{V}_i t)$, where t is a time. In the present linear system the correction due to the additional unsteady but spatially uniform term in the boundary condition at infinity is simply expressed by superposition of the solution of the corresponding boundary-value problem of the Boltzmann and heat equations (with additional time-derivative terms). The solution, which is obviously a function of t and r only, does not contribute to the force on the particle. However, when the heat capacity of the particle is very large ($\beta \mathrm{C}/\mathrm{R}\rho_0\mathrm{L}^3 \gg 1$, where C is the heat capacity of the particle), the temperature rise in the particle owing to the heat transferred from the surrounding gas is so small that the temperature difference of the particle and the surrounding gas increases with time and becomes too large for the linearized theory to be applied. The function $h_\mathrm{T}/h_\mathrm{D}$ of k in the formula (57) of the thermophoretic velocity V_i is shown in Fig. 16, where various experimental data are also shown for comparison. The data in Ref. 35 are scattered; the data in Refs. 30 and 36 are fairly close to our numerical results.

Finally, it is noted that some of the experimental results shown in Figs. 15 and 16 are those in air, which is not a single component monoatomic gas dealt with in our analysis.

VII. Summary

In the present paper we first investigated a flow induced around a sphere with a nonuniform surface temperature in a rarefied gas, mainly numerically, on the basis of the linearized Boltzmann equation for hard-sphere molecules. The flow field, the velocity distribution function as well as the macroscopic variables, and the force on the sphere are obtained accurately for the whole range of the Knudsen number. Then we considered the drag and thermal force problems of a spherical particle with an arbitrary thermal conductivity. The solutions were shown to be constructed by appropriate superpositions of the solution of the problem of nonuniform temperature sphere and the solutions of the drag and thermal force problems of a sphere with a uniform temperature. Necessary formulas and numerical data to obtain the solutions, especially those for the drag, thermal force, and thermophoretic velocity, were prepared.

REFERENCES

1. Y. Sone, *Rarefied Gas Dynamics*, (Eds. L. Trilling and H. Y. Wachman, Academic, New York, 1969), Vol. 1, p. 243.
2. Y. Sone, *Rarefied Gas Dynamics*, (Ed. D. Dini, Editrice Tecnico Scientifica, Pisa, 1971), Vol. 2, p. 737.
3. Y. Sone and K. Aoki, *Transp. Theory Stat. Phys.*, **16**, 189 (1987); *Mem. Fac. Eng., Kyoto Univ.*, **49**, 237 (1987).
4. Y. Sone, *Advances in Kinetic Theory and Continuum Mechanics*, (Eds. R. Gatignol and Soubbaramayer, Springer-Verlag, Berlin, 1991), p. 19.
5. Y. Sone and K. Aoki, *Molecular Gas Dynamics*, (Asakura, 1994), Chap. III (in Japanese).
6. E. H. Kennard, *Kinetic Theory of Gases*, (McGraw-Hill, New York, 1938), Chap. VIII, Sec. 184.
7. Y. Sone, *J. Phys. Soc. Jpn.*, **21**, 1836 (1966).
8. T. Ohwada, Y. Sone, and K. Aoki, *Phys. Fluids A*, **1**, 1588 (1989).
9. Y. Sone, *Phys. Fluids*, **15**, 1418 (1972).
10. T. Ohwada and Y. Sone, *Eur. J. Mech., B/Fluids*, **11**, 389 (1992).

11. M. N. Kogan, V. S. Galkin, and O. G. Fridlender, *Sov. Phys. Usp.*, **19**, 420 (1976).

12. S. Takata, Y. Sone, and K. Aoki, *Phys. Fluids A*, **5**, 716 (1993).

13. M. Knudsen and S. Weber, *Ann. Phys. (Leipzig)*, **36**, 981 (1911).

14. R. A. Millikan, *Phys. Rev.*, **32**, 349 (1911).

15. R. A. Millikan, *Phys. Rev.*, **22**, 1 (1923).

16. P. S. Epstein, *Phys. Rev.*, **23**, 710 (1924).

17. R. Goldberg, *Ph. D. thesis*, New York Univ. (1954).

18. A. B. Basset, *Hydrodynamics*, (Dover, New York, 1961), Vol. II, p. 270.

19. D. R. Willis, *Phys. Fluids*, **9**, 2522 (1966).

20. C. Cercignani, C. D. Pagani, and P. Bassanini, *Phys. Fluids*, **11**, 1399 (1968).

21. W. F. Phillips, *Phys. Fluids*, **18**, 1089 (1975).

22. K. C. Lea and S. K. Loyalka, *Phys. Fluids*, **25**, 1550 (1982).

23. S. P. Bakanov, V. V. Vysotskij, B. V. Derjaguin, and V. I. Roldughin, *J. Non-Equilib. Thermodyn.*, **8**, 75 (1983).

24. W. S. Law and S. K. Loyalka, *Phys. Fluids*, **29**, 3886 (1986).

25. K. Aoki and Y. Sone, *Phys. Fluids*, **30**, 2286 (1987).

26. S. A. Beresnev, V. G. Chernyak, and G. A. Fomyagin, *J. Fluid Mech.*, **219**, 405 (1990).

27. S. K. Loyalka, *Phys. Fluids A*, **4**, 1049 (1992).

28. P. S. Epstein, *Z. Phys.*, **54**, 537 (1929).

29. S. P. Bakanov and B. V. Deryaguin, *Kolloidnyi Zhurnal*, **21**, 377 (1959).

30. K. H. Schmitt, *Z. Naturforsch.*, **14a**, 870 (1959).

31. L. Waldmann, *Z. Naturforsch.*, **14a**, 589 (1959).

32. C. F. Schadt and R. D. Cadle, *J. Phys. Chem.*, **65**, 1689 (1961).

33. J. R. Brock, *J. Colloid Sci.*, **17**, 768 (1962).

34. S. Jacobsen and J. R. Brock, *J. Colloid Sci.*, **20**, 544 (1965).

35. B. V. Derjaguin, A. I. Storozhilova, and Ya. I. Rabinovich, *J. Colloid Interface Sci.*, **21**, 35 (1966).

36. W. F. Phillips, *Phys. Fluids*, **18**, 144 (1975).

37. F. Prodi, G. Santachiara, and V. Prodi, *J. Aerosol Sci.*, **10**, 421 (1979).

38. S. P. Bakanov, B. V. Deryagin, and V. I. Roldugin, *Sov. Phys. Usp.*, **22**, 813 (1979),

39. Y. Sone and K. Aoki, *Rarefied Gas Dynamics*, (Ed. S. S. Fisher, AIAA, New York, 1981), Part I, p. 489.

40. L. Talbot, *Rarefied Gas Dynamics*, (Ed. S. S. Fisher, AIAA, New York, 1981), Part I, p. 467.

41. Y. Sone and K. Aoki, *J. Méc. Théor. Appl.*, **2**, 3 (1983).

42. S. A. Beresnev and V. G. Chernyak, *Sov. Phys. Dokl.*, **30**, 1055 (1985).

43. K. Yamamoto and Y. Ishihara, *Phys. Fluids*, **31**, 3618 (1988).

44. S. P. Bakanov, *Aerosol Science and Technology*, **15**, 77 (1991).

45. S. K. Loyalka, *J. Aerosol Sci.*, **23**, 291 (1992).

46. S. Takata, Y. Sone, and K. Aoki, *J. Aerosol Sci.*, **24**, S147 (1993).

47. S. Takata, K. Aoki, and Y. Sone, *Rarefied Gas Dynamics*, (Eds. B. D. Shizgal and D. P. Weaver, AIAA, Washington D. C., 1994), p. 626.

48. Y. Sone and K. Aoki, *Rarefied Gas Dynamics*, (Ed. J. L. Potter, AIAA, New York, 1977), Part 1, p. 417.

49. Y. Sone and K. Aoki, *Phys. Fluids*, **20**, 571 (1977).

50. K. Aoki, T. Inamuro, and Y. Onishi, *J. Phys. Soc. Jpn.*, **47**, 663 (1979).

51. S. K. Loyalka, *Progress in Nuclear Energy*, **12**, 1 (1983).

52. S. Takata, Y. Sone, and K. Aoki, *J. Vac. Soc. Jpn.*, **35**, 143 (1992), (in Japanese).

53. S. Takata and Y. Sone, *J. Vac. Soc. Jpn.*, **37**, 151 (1994), (in Japanese).

54. H. Grad, *Rarefied Gas Dynamics*, (Ed. J. A. Laurmann, Academic, New York, 1963), Vol. 1, p. 26.

55. C. Cercignani, *The Boltzmann Equation and Its Applications*, (Springer-Verlag, Berlin, 1988), Chap. IV, Sec. 5.

56. Y. Sone and S. Takata, *Transp. Theory Stat. Phys.*, **21**, 501 (1992).

57. Y. Sone, T. Ohwada, and K. Aoki, *Phys. Fluids A*, **1**, 363 (1989).

58. Y. Sone, *J. Méc. Théor. Appl.*, **3**, 315 (1984).

59. Y. Sone, *J. Méc. Théor. Appl.*, **4**, 1 (1985).

60. K. Aoki, Y. Sone, and T. Ohwada, *Rarefied Gas Dynamics*, (Eds. V. Boffi and C. Cercignani, Teubner, Stuttgart, 1986), Vol. I, p. 236.

61. Y. Sone, *Phys. Fluids*, **16**, 1422 (1973).

62. P. L. Bhatnagar, E. P. Gross, and M. Krook, *Phys. Rev.*, **94**, 511 (1954).

63. P. Welander, *Ark. Fys.*, **7**, 507 (1954).

64. M. N. Kogan, *Appl. Math. Mech.*, **22**, 597 (1958).

65. Y. Sone and S. Tanaka, *Rarefied Gas Dynamics*, (Eds. V. Boffi and C. Cercignani, Teubner, Stuttgart, 1986), Vol. I, p. 194.

66. C. L. Pekeris and Z. Alterman, *Proc. Natl. Acad. Sci. U.S.A.*, **43**, 998 (1957).

67. H. Chihara, private communication, (1990).

TABLE I. Force on the sphere: h vs k [*cf.* Eq. (22a)].

k	$h(k)$	$\Delta h(k)$*	k	$h(k)$	$\Delta h(k)$
0	0.0000	–	1	–0.7908	0.0006
0.05	–0.0228	0.0005	2	–0.9327	0.0004
0.1	–0.0788	0.0008	4	–0.9994	0.0003
0.2	–0.2241	0.0015	6	–1.0187	0.0002
0.4	–0.4694	0.0007	10	–1.0321	0.0001
0.6	–0.6254	0.0008	∞	–1.0472	–

* $\Delta h(k)$ means the variation (max–min) of $h(k)$ computed on the control spheres $r = r^{(i)}$ for all the lattice points $r^{(i)}$ between $r = 1$ and 4.

TABLE II. Fundamental data for the drag and thermal force on a spherical particle with an arbitrary thermal conductivity: $h_{\rm D}(\lambda_p = \infty)$, $h_{\rm T}(\lambda_p = \infty)$, and h and $Q_{r{\rm D}}(\lambda_p = \infty)|_{r=1}/u_\infty \cos\theta$, $Q_{r{\rm T}}(\lambda_p = \infty)|_{r=1}/(5/4)k\gamma_2\beta\cos\theta$, and $Q_r|_{r=1}/\alpha\cos\theta$. From these data, the drag and thermal force on a spherical particle with an arbitrary thermal conductivity can be obtained with Eqs. (51a)–(51c) and (52a)–(52c).

k	$h_{\rm D}(\lambda_p = \infty)$	$\dfrac{Q_{r{\rm D}}(\lambda_p = \infty)\|_{r=1}}{u_\infty \cos\theta}$	$h_{\rm T}(\lambda_p = \infty)$	$\dfrac{Q_{r{\rm T}}(\lambda_p = \infty)\|_{r=1}}{(5/4)k\gamma_2\beta\cos\theta}$	h	$\dfrac{Q_r\|_{r=1}}{\alpha\cos\theta}$
0	0.0000	0.0000*	0.0000	–3.0000*	0.0000	0.0000
0.05	1.1091	0.0053	–0.0068	–2.3955	–0.0228	0.1859
0.1	2.1168	0.0189	–0.0457	–1.9797	–0.0788	0.2952
0.15	–	–	–0.1145	–1.6935	–	–
0.2	3.8110	0.0535	–0.2075	–1.4911	–0.2241	0.4048
0.3	–	–	–0.4124	–1.2319	–	–
0.4	6.2292	0.1118	–0.6017	–1.0766	–0.4694	0.4819
0.6	7.7951	0.1492	–0.9034	–0.9025	–0.6254	0.5097
1	9.5625	0.1887	–1.2585	–0.7500	–0.7908	0.5318
2	11.2772	0.2226	–1.6001	–0.6282	–0.9327	0.5480
4	12.2333	0.2386	–1.7818	–0.5649	–0.9994	0.5561
6	12.5557	0.2432	–1.8399	–0.5435	–1.0187	0.5588
10	12.8071	0.2464	–1.8838	–0.5262	–1.0321	0.5609
∞	13.1653	0.2500*	–1.9423	–0.5000*	–1.0472	0.5642

* The analytical solutions for small and infinite k can be obtained as follows: for small k

$$\frac{Q_{r{\rm D}}(\lambda_p = \infty)|_{r=1}}{u_\infty \cos\theta} = \left[\frac{3}{2}\gamma_3 - 3\int_0^\infty {\rm H_A}(\eta)d\eta\right]k^2, \qquad \frac{Q_{r{\rm T}}(\lambda_p = \infty)|_{r=1}}{(5/4)k\gamma_2\beta\cos\theta} = -3 - 6d_1 k,$$

and for infinite k

$$\frac{Q_{r{\rm D}}(\lambda_p = \infty)|_{r=1}}{u_\infty \cos\theta} = \frac{1}{4}, \qquad \frac{Q_{r{\rm T}}(\lambda_p = \infty)|_{r=1}}{(5/4)k\gamma_2\beta\cos\theta} = -\frac{1}{2},$$

where $\gamma_3 = 1.947906$ (hard sphere), 1 (BKW) and ${\rm H_A}(\eta)$ is a Knudsen-layer function in the shear flow[8,5].

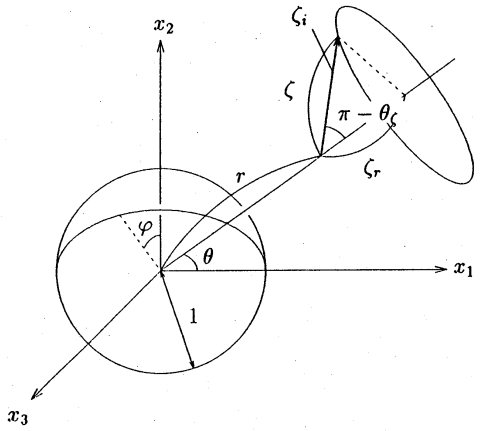

Fig. 1. Geometry and coordinate systems.

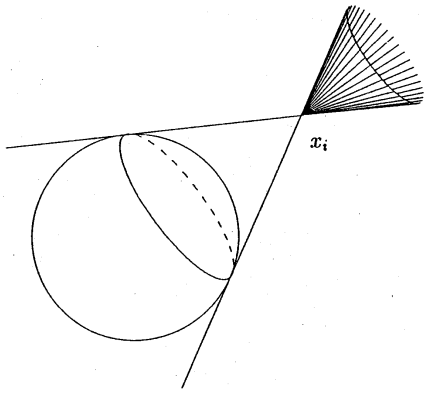

Fig. 2. Discontinuity of the velocity distribution function. At the point x_i, the velocity distribution function is discontinuous on the shaded cone in ζ_i space.

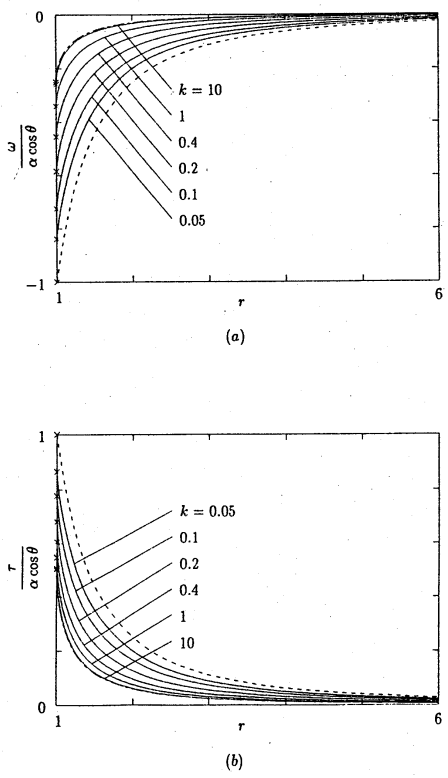

Fig. 3. Density and temperature field: (a) $\omega/\alpha\cos\theta$, (b) $\tau/\alpha\cos\theta$. Here, —— indicates the present numerical result, - - - - the Stokes solution without slip ($k = 0$), and – – – the free molecular solution ($k = \infty$). The values on the sphere are marked by ×.

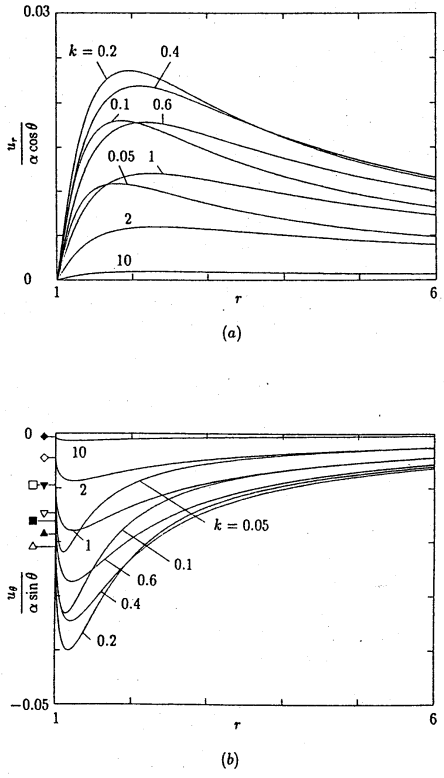

Fig. 4. Velocity field: (a) $u_r/\alpha\cos\theta$, (b) $u_\theta/\alpha\sin\theta$. Here, —— indicates the present numerical result. The flow vanishes for the Stokes solution without slip ($k = 0$) and the free molecular solution ($k = \infty$). The values on the sphere are marked by □ for $k = 0.05$, ■ for $k = 0.1$, △ for $k = 0.2$, ▲ for $k = 0.4$, for ▽ $k = 0.6$, ▼ for $k = 1$, ◇ for $k = 2$, and ◆ for $k = 10$ in (b).

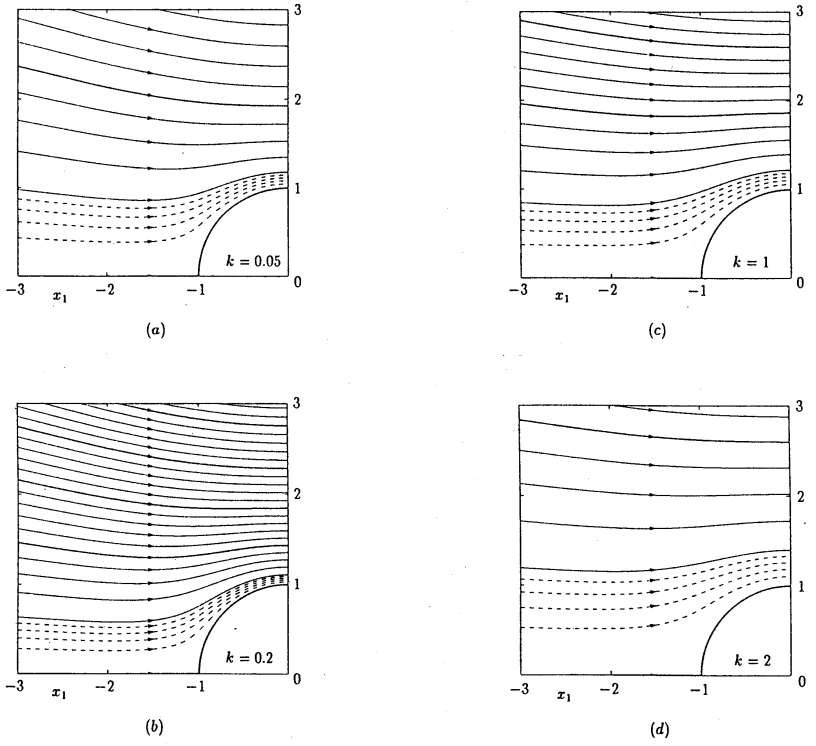

Fig. 5. Streamlines of the flow (in a plane including the x_1 axis): (*a*) $k = 0.05$, (*b*) $k = 0.2$, (*c*) $k = 1$, and (*d*) $k = 2$. The streamlines $\Psi/\alpha = 4 \times 10^{-3} n$, ($n = 0, 1, 2, \cdots$) are shown in solid lines, the thick lines of which indicate the case $n = 0, 5, 10, \cdots$, and the lines $\Psi/\alpha = 4 \times 10^{-3}(n/5)$, ($n = 1, 2, 3,$ and 4) are shown by dashed lines, where Ψ is the Stokes's stream function defined by $u_r = (r^2 \sin\theta)^{-1} \partial\Psi/\partial\theta$, $u_\theta = -(r \sin\theta)^{-1} \partial\Psi/\partial r$. The streamline closer to the sphere takes the smaller value of Ψ/α; $\Psi/\alpha = 0$ for the line on the x_1 axis. The arrows indicate the direction of the flow for $\alpha > 0$.

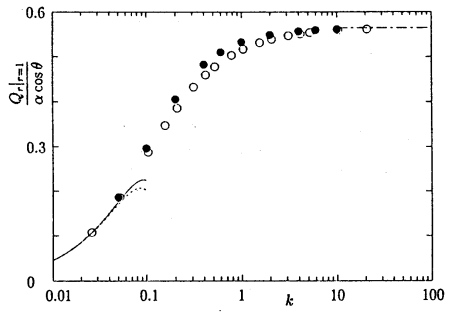

Fig. 6. Heat flow on the sphere: $Q_r|_{r=1}/\alpha \cos\theta$ vs k. Here, ● indicates the present result for hard-sphere molecules, ○ the present result for the BKW model, —— the asymptotic solution for hard-sphere molecules [Eq. (31)], ---- the asymptotic solution for the BKW model [Eq. (31)], and —·— the free molecular solution ($k = \infty$).

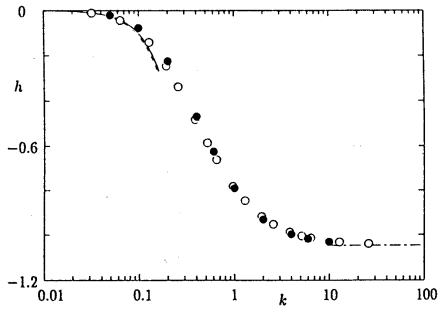

Fig. 7. Force on the sphere: h vs k [*cf.* Eq. (22a)]. Here, ● indicates the present result for hard-sphere molecules, ○ the present result for the BKW model [Eq. (32)], —— the asymptotic solution for hard-sphere molecules [Eq. (32)], ---- the asymptotic solution for the BKW model, and —·— the free molecular solution ($k = \infty$).

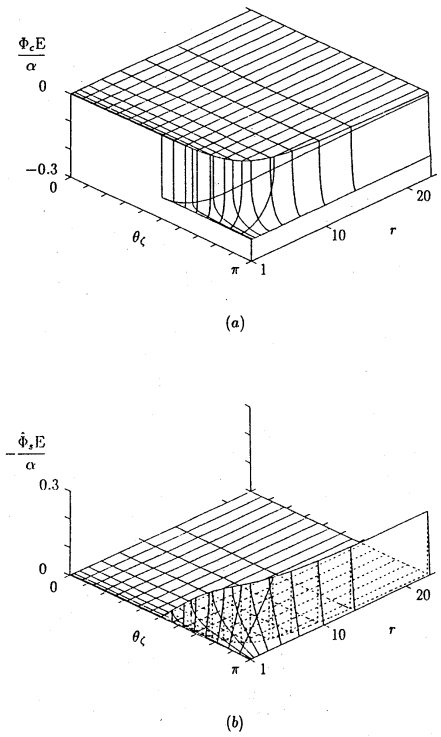

Fig. 8. Velocity distribution functions $\Phi_c E$ and $\hat{\Phi}_s E$ at $\zeta = 0.556$ for the free molecular flow ($k = \infty$) [Eqs. (26a) and (26b)]. (*a*) $\Phi_c E$ and (*b*) $\hat{\Phi}_s E$. The $\Phi_c E$ and $\hat{\Phi}_s E$ are shown as functions of r and θ_ζ by lines r = const and θ_ζ = const on the surfaces. The vertical lines show the discontinuity at $r \sin\theta_\zeta = 1$. The invisible lines behind other parts are shown by dashed lines.

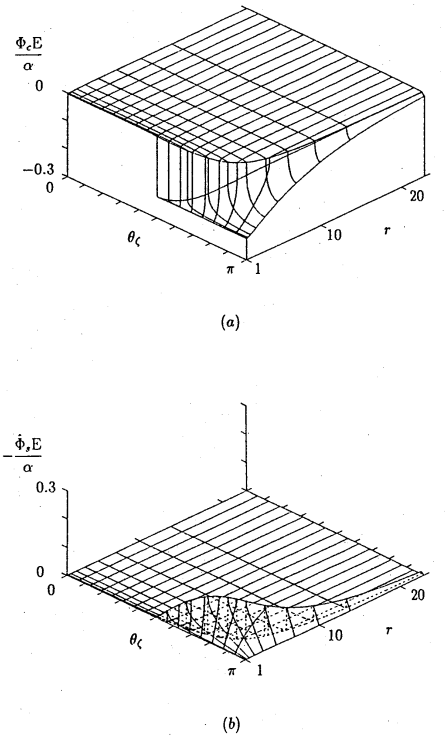

Fig. 9. Velocity distribution functions $\Phi_c E$ and $\hat{\Phi}_s E$ at $\zeta = 0.556$ for $k = 10$. (*a*) $\Phi_c E$ and (*b*) $\hat{\Phi}_s E$. (See the caption of Fig. 8.)

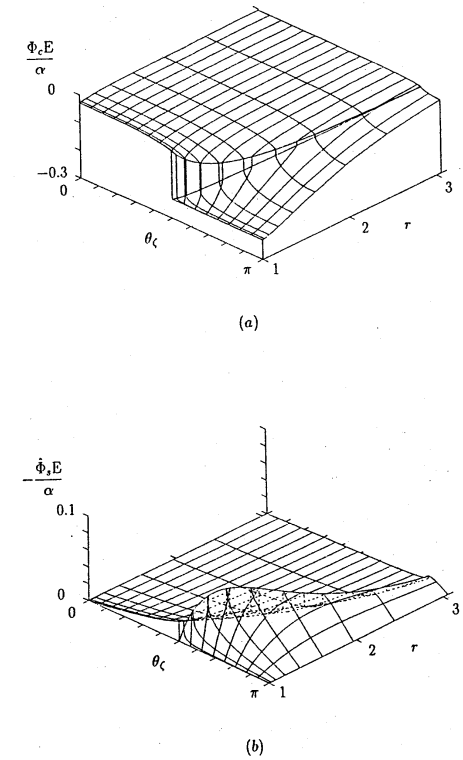

Fig. 10. Velocity distribution functions $\Phi_c E$ and $\hat{\Phi}_s E$ at $\zeta = 0.556$ for $k = 1$. (*a*) $\Phi_c E$ and (*b*) $\hat{\Phi}_s E$. (See the caption of Fig. 8.)

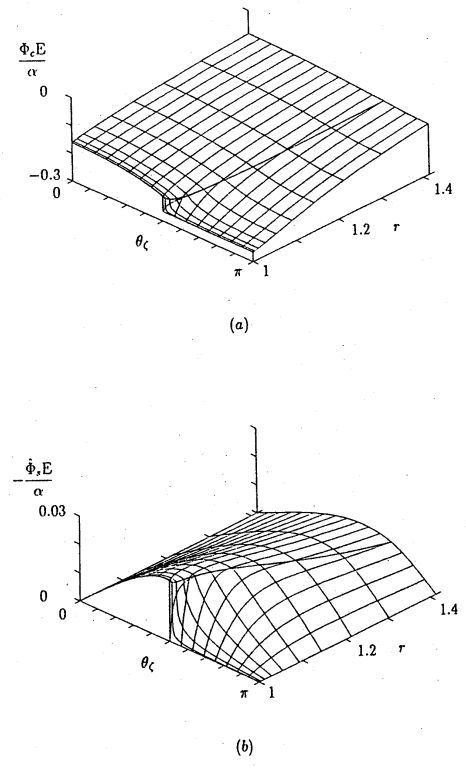

Fig. 11. Velocity distribution functions $\Phi_c E$ and $\hat{\Phi}_s E$ at $\zeta = 0.556$ for $k = 0.1$. (*a*) $\Phi_c E$ and (*b*) $\hat{\Phi}_s E$. (See the caption of Fig. 8.)

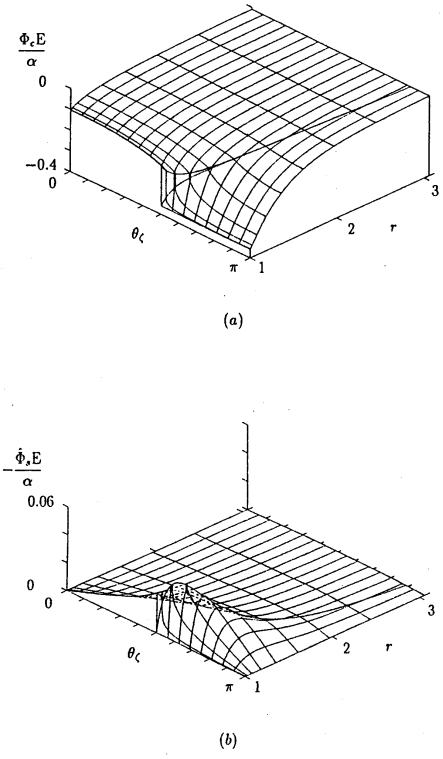

Fig. 12. Velocity distribution functions $\Phi_c E$ and $\hat{\Phi}_s E$ at $\zeta = 0.139$ for $k = 1$. (*a*) $\Phi_c E$ and (*b*) $\hat{\Phi}_s E$. (See the caption of Fig. 8.)

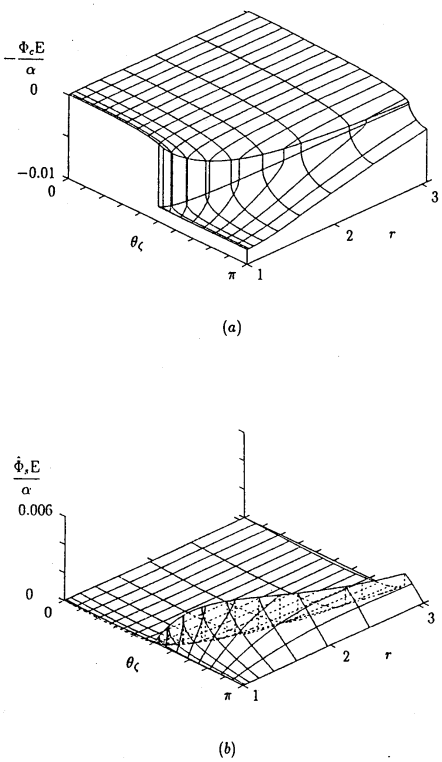

Fig. 13. Velocity distribution functions $\Phi_c E$ and $\hat{\Phi}_s E$ at $\zeta = 1.70$ for $k = 1$. (*a*) $\Phi_c E$ and (*b*) $\hat{\Phi}_s E$. (See the caption of Fig. 8.)

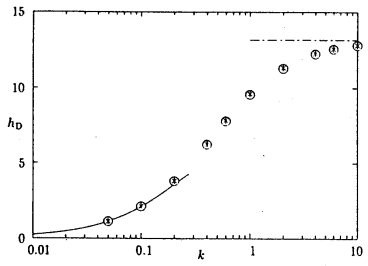

Fig. 14. Drag $p_0 L^2 U_{\infty i} (2RT_0)^{-1/2} h_D$ on a spherical particle with an arbitrary thermal conductivity: h_D vs k. Here, ○ indicates the numerical result for $\lambda_p/\lambda_g = \infty$, ∗ for 1. The solid line —— indicates the asymptotic solution [Eq. (55)], and – – – the free molecular solution ($k = \infty$) [Eq. (53)]; they are independent of λ_p/λ_g.

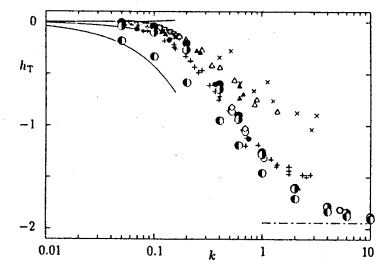

Fig. 15. Thermal force $(2RT_0)^{-1/2} L^2 \lambda_g (\partial T/\partial X_i)_\infty h_T$ on a spherical particle with an arbitrary thermal conductivity: h_T vs k. Here, ● indicates the numerical result for $\lambda_p/\lambda_g = \infty$, for ◑ 10, for ◐ 1. The solid lines —— indicate the asymptotic solutions for small k {from the top, $\lambda_p/\lambda_g = \infty$ (correct up to $O(k^2)$[10]), 10 and 1 [Eq. (56)]}, and – – – indicates the free molecular limit ($k \to \infty$) [Eq. (54)]. Experimental results by several authors are indicated by smaller markers: × indicates the case $\lambda_p/\lambda_g = 475$ (Hg in Air), △ 263 (NaCl in Air), ▲ 8.14 (tricresyl phosphate in Air) in Ref. 32; ▽ 366 (NaCl in Ar) in Ref. 34; • 8.14 (tricresyl phosphate in Air) in Ref. 36; + 7.41 (Oil in Ar) in Ref. 30. Numerical results in Ref. 45 are also indicated by small markers: ◇ and ○ indicate $\lambda_p/\lambda_g = 100$ and 10 respectively.

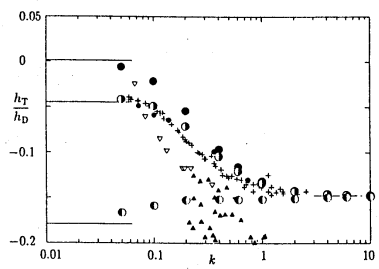

Fig. 16. Thermophoretic velocity $\lambda_g p_0^{-1} (\partial T/\partial X_i)_\infty (h_T/h_D)$ of a spherical particle with an arbitrary thermal conductivity: h_D/h_T vs k. Here, ● indicates the numerical result for $\lambda_p/\lambda_g = \infty$, ◑ for 10, ◐ for 1. The solid lines —— indicate the asymptotic solutions for small k {from the top, $\lambda_p/\lambda_g = \infty$, 10, and 1 [the leading term obtained from Eq. (73) in Ref. 10 or Eq. (56) and Eq. (55)]}; and – – – indicates the free molecular limit ($k \to \infty$) [obtained from Eqs. (53) and (54)]. Experimental results by several authors are indicated by smaller markers: ▲ 5.22 (Vaseline oil in Air) in Ref. 35; ▽ 256 (NaCl in Air) in Ref. 37; • 8.14 (tricresyl phosphate in Air) in Ref. 36; + 7.41 (Oil in Ar) in Ref. 30.